This article is part of the

Proceedings of the 16th Minisymposium Verfahrenstechnik and 7th Partikelforum (TU Wien, Sept. 21/22, 2020)

Title:
DEVELOPMENT AND CHARACTERIZATION OF CARBON SUPPORTED PALLADIUM-BASED ANODE CATALYSTS FOR THE ALKALINE DIRECT ETHANOL FUEL CELL

Corresponding author:
Sigrid Wolf (TU Graz), sigrid.wolf@tugraz.at

Date of submission:
28.02.20

Date of revision:
01.09.20

Date of acceptance:
09.09.20

Chapter ID:
DiP3-(02)

Length:
6 pages

ISBN (full book):
978-3-903337-01-5

Development and Characterization of Carbon Supported Palladium Based Anode Catalysts for the Alkaline Direct Ethanol Fuel Cell

Sigrid Wolf[1,*], Michaela Roschger[1], Viktor Hacker[1]
1: Technical University of Graz, Institute for Chemical Engineering and Environmental Technology, Inffeldgasse 25/C, 8010 Graz, Austria
*Sigrid.Wolf@TUGraz.at

Keywords: Direct ethanol fuel cell, Anode catalysts, Alkaline ethanol oxidation reaction, Rotating disk electrode analysis.

Abstract

Direct ethanol fuel cells (DEFC) are limited by the slow kinetics of the ethanol oxidation reaction (EOR) at the anode. In this work, a ternary PdNiBi/C catalyst was synthesized via the modified instant method including a few modifications to investigate the influence on the performance for the alkaline EOR. The catalyst was ex-situ characterized by means of thin film rotating disk electrode technique using a standard three electrode set-up. The results were compared with a commercial Pd/C catalyst. With the CV measurements, all characteristic reduction and oxidation peaks for Pd, Ni, and Bi as well as for the hydrogen ad/absorption were observed. The PdNiBi/C (636 $cm^2\ mg^{-1}$) catalyst presents a higher EASA than the commercial Pd/C (411 $cm^2\ mg^{-1}$). The onset potential of the ternary catalyst (0.193 V) is lower, the maximum current density (138 mA cm^{-2}) of the forward scan is higher and a better byproduct tolerance is examined compared to the commercial catalyst (0.255 V, 126 mA cm^{-2}). The remaining current density of the PdNiBi/C is 13 % higher than that of the commercial Pd/C.

Introduction

In recent years, demand of renewable energy has been increasing due to the limitation of fossil fuels and large CO_2 emission. Fuel cells are identified as one of key technologies for clean energy industry of the future [1, 2]. However, there are three critical technical barriers, which limit the commercialization of fuel cells: a) performance (activity), b) durability (stability), and c) costs [3, 4]. Direct ethanol fuel cells (DEFC) have attracted attention in the last decades due to their easy handling, low cost and environmental friendliness [5, 6]. In addition, ethanol shows relatively high energy densities (8.01 kWh kg^{-1}) that are comparable to gasoline (11 kWh kg^{-1}) [7].

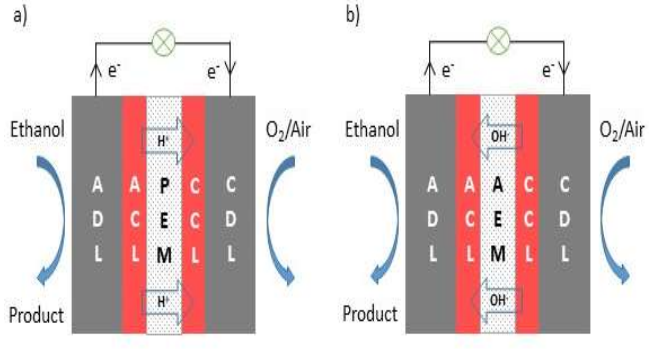

Figure 1: Schematic illustration of a) proton exchange membrane (PEM) and b) anion exchange membrane (AEM) direct ethanol fuel cell with cathode catalyst layer (CCL), anode catalyst layer (ACL), cathode diffusion layer (CDL) and anode diffusion layer (ADL) (adapted from [4]).

However, DEFCs are limited by the slow kinetics, especially of the electrochemical reaction at the anode and the ethanol crossover through the membrane from the anode to the cathode. The crossover is causing a mixed potential thus resulting in a reduction of the cathode potential. Consequently, these both limitations contribute drastically to the power density decrease of alkaline DEFC systems. Therefore, the transition from acidic to alkaline electrolyte became more important to improve the kinetics of the alcohol oxidation reaction and oxygen reduction reaction [8, 9].

In alkaline DEFC, an Anion Exchange Membrane (AEM) is used to transfer anions (e.g. OH^-, CO_3^{2-} and/or HCO_3^-), whereas in acidic DEFC, a Proton Exchange Membrane (PEM), mostly Nafion 115® or Nafion 117®, is applied for the movement of cations (e.g. H^+ or Na^+).

The dragging force of the moving ions in AEM is reversed to PEM, reducing problems of fuel crossover. Another advantage of alkaline DEFC is the simplified water management.

The most used catalyst for alcohol oxidation is platinum, but high cost, low availability and prevalent poisoning by adsorbed CO-like intermediates formed during ethanol oxidation limits its application. Alkaline DEFC show faster kinetics due to high concentration of OH- ions [4, 6, 10]. Hence, cost efficient Pt catalysts can be substituted by more abundant, cheaper and non-noble metal containing catalysts.

Currently, palladium is the most suitable catalyst for the replacement of platinum in DEFC. Ma et al. [11] have reported that Pd/C catalysts exhibit a higher ethanol oxidation reaction (EOR) activity than Pt/C in alkaline condition. This can be attributed to higher oxophilic characteristics and the inherent ability of Pd on C-C bond cleavage. This positive effect also causes a higher stability and less susceptibility to poisoning of the active sides of the Pd catalyst during EOR [5, 11, 12].

However, the complete oxidation of ethanol remains as main challenge for DEFC development. As it can be seen in equation 1, the complete ethanol oxidation leads to CO_2 and water with the release of $12e^-$. In comparision, state-of-the-art catalyst systems lead to an incomplete oxidation reaction resulting in acetic acid (acetate) with $4e^-$ released as described in equation 2 [4].

Complete oxidation:

$$CH_3CH_2OH + 12OH^- \rightarrow 2CO_2 + 9H_2O + 12e^- \quad (1)$$

Incomplete oxidation:

$$CH_3CH_2OH + 5OH^- \rightarrow CH_3COO^- + 4H_2O + 4e^- \quad (2)$$

The cleavage of the C-C bond of ethanol resulting in a CO_2 efficiency of 100% can be described by the C_1 pathway, but the ethanol oxidation reaction in alkaline media with currently available catalysts predominantly follows the C_2 pathway (Figure 2). Ethanol is oxidized by hydroxide ions to acetic acid/acetate as the main oxidation products. During the EOR, acetate is adsorbed on the catalyst surface as the active species. Nevertheless, various reaction intermediates deactivate the catalyst due to poisoning of the active sites and thus decrease the EOR performance [13, 14].

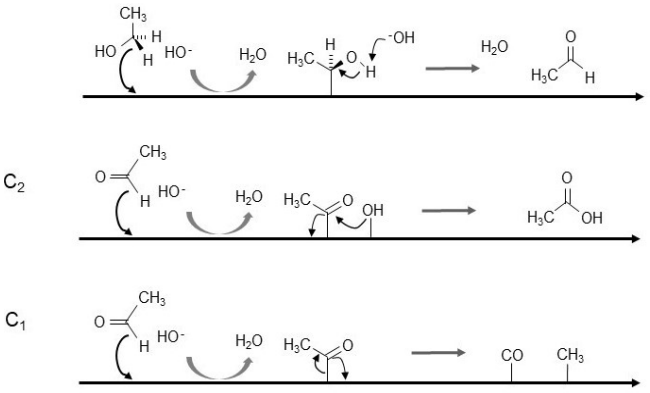

Figure 2: Alkaline EOR: C2 pathway and C1 pathway [14].

The reaction mechanism of EOR for Pd-based catalystsis still not completely explained. Multiple studies [12, 15, 16] describe the generally accepted mechanism of EOR on Pd in alkaline media as followed in Equations 3-7:

$$Pd^0 + OH^- \leftrightarrows Pd\text{-}OH_{ads} + e^- \quad (3)$$

$$Pd^0 + CH_3CH_2OH \leftrightarrows Pd\text{-}(CH_3CH_2OH)_{ads} \quad (4)$$

$$Pd\text{-}(CH_3CH_2OH)_{ads} + 3OH^- \leftrightarrows Pd\text{-}(COCH_3)_{ads} + 3H_2O + 3e^- \quad (5)$$

$$Pd\text{-}(COCH_3)_{ads} + Pd\text{-}OH_{ads} \leftrightarrows Pd\text{-}(CH_3COOH)_{ads} + Pd^0 \quad (6)$$

$$Pd\text{-}(CH_3COOH)_{ads} + OH^- \leftrightarrows Pd^0 + CH_3COO^- + H_2O \quad (7)$$

From this reaction pathway, the importance of the OH^- ions for the conversion of the intermediates (acyl) to acetate is pointed out. Liang et al. [16] describe that the removal of the adsorbed acyl by the adsorbed hydroxyl is the rate determining step (equation 6), while the dissociative adsorption of ethanol is quickly proceeded [12, 17, 18].

In the last years, a lot of research is dedicated to anode materials to enhance the EOR performance and to reduce the costs of the fuel cell. The two most promising techniques for that are first, to find appropriate synthesis methods for catalyst nanostructures to enlarge the surface area of the active material and second, to alloy Pd with other metals. The advantage of bi- and trimetallic catalysts is that the additives are mainly cheaper and act as co-catalysts which facilitate the catalytic activity [1, 8].

Ni is a very promising candidate as co-catalyst for Pd. It causes the formation of alloys thus resulting in a shift of the lattice constants and promotes synergetic effects. The binding energy at the surface is lowered and therefore, the poisoning effect by different adsorbents like CO or CH_x species is reduced [19, 20, 21]. Moreover, Ni has a high affinity for the attraction of OH^--ions, that are fundamental for the EOR as described above [2].

In contrast to Ni, Bi and Pd have quite different crystallographic properties, which significantly reduces the probability of alloy formation [22]. Nevertheless, Neto et al. [23] reported a positive impact on the performance of the anode catalyst upon adding Bi to Pd. Additionally, crystallographic changes were observed during the synthesis. Huang et al. [24] describe the affinity of Pd to Bi(III)-ions that are adsorbed on the surface as one possibility for the interaction. In literature, the formation of oxide- and hydroxide-species at the surface is also said to increase the OH^- concentration at the catalyst surface and thus enhances the activity for EOR [23, 24, 25].

Another strategy to enhance the electrocatalytic activity of the Pd catalysts is the deposition of the nanoparticles on a suitable support material [1, 8]. The dispersion of the active material on a support results in a higher active surface area and thus the total loading can be reduced that further lowers the costs [26]. The most used supports are carbon based materials (e.g. Vulcan XC72R from Carbot Cooperation) that show an excellent combination of surface properties, electronic conductivity and corrosion resistance. Therefore, it is well known, that the support material influences the particle size, morphology, particle distribution and stability [27, 28].

As it can be seen in equation 3-7, the EOR on Pd is a typical multistep and multiselective catalytic process with a complex network of steps. Pd catalysts can greatly influence its EOR performance due to various atomistic properties and adsorption behaviours of different Pd crystal facets [29]. The Pd (100) crystal structure is proved to be the best surface for ethanol dissociation with relatively low energy barriers [15, 29]. The shape of the nanoparticles is another critical factor for the catalytic activity, because the shape is in correlation with the surface structure. Hao et al. [30] reported a higher activity of cubic Pd nanocrystals than for the spherical ones. This can be attributed to a higher concentration of the more active Pd (100) facets in the cubic nanoparticles. Another critical factor that effects the catalytic activity of the nanoparticles is the particle size. The reduction of the particle size results in a higher surface area and thus increases the quantity of available active atoms [31].

Therefore, many research groups focused on the development of a suitable synthesis method of nanoelectrocatalysts [31, 32]. The chemical reduction method is a facile strategy for the synthesis of mono-, bimetallic or ternary catalysts. Various reducing agents like sodium borohydride hydrazine alcohols, citric acid and ascorbic acid have been used for the reduction of the metals [31].

In this study, a carbon supported ternary PdNiBi catalyst is synthesized by the modified instant method [13] and compared with a commercial Pd/C catalyst from fuel cell store. The prepared and commercial catalysts were ex-situ characterized by means of thin film rotating disk electrode technique using a standard three electrode set-up. Cyclic voltammetry (CV) and EOR measurements were recorded in N_2 purged potassium hydroxide solution (1 M) and a mixture of potassium hydroxide and ethanol solution (1 M), respectively. The obtained data are utilised to determine the electrochemical active surface area (EASA), the EOR activity and the byproduct tolerance of the catalysts. Chronoamperometry was performed to examine the stability of the catalysts.

Materials and Methods

Materials. Carbon Black (XC72R, Carbot), Palladium (II) chloride ($PdCl_2$, anhydrous, 59-60% Pd basis, Sigma Aldrich), Nickel (II) nitrate hexahydrate ($Ni(NO_3)_2 \cdot 6\ H_2O$, 99 % trace metals basis, Sigma Aldrich), Bismuth (III) chloride ($BiCl_3$, ≥ 98 % p.a., Sigma Aldrich), Sodium Hydroxide (NaOH, 98 % p.a., Baker), Sodium borohydride ($NaBH_4$, ≥ 98 % p.a., Sigma Aldrich), Ethanol (EtOH, 99.9 % p.a., Roth), Propanol-2 (Isopropanol, 99.9 % p.a., Roth), Potassium Hydroxide (KOH, 1.0 M Fixanal 1 L Ampoule, Sigma Aldrich), Hydrochloric acid (HCl, 37 % p.a., Roth), Nafion® Solution (5 wt% in H_2O, Quintech), Alumina suspension (Al_2O_3, 0.05 µm, MasterPrep Bühler).

Pd-based Nanocatalyst Preparation using Modified Instant Method. The carbon supported PdNiBi catalyst was synthesized based on the modified instant method [33]. The catalyst was prepared using Vulcan XC72R as a carbon support with the following metal loading: 60 wt % carbon and 40 wt% metal. First, an appropriate amount of Vulcan XC72R

was dispersed in 60 mL of ultrapure water. An ultrasonic probe (Hirscher, UP400s) was used for sonication at an amplitude of 40 % and a cycle of 1 (5 minutes, two times) under nitrogen atmosphere and ice cooling.
Three metal precursor salt solutions are separately prepared by adding 10 mL ultrapure water to an appropriate amount of the $PdCl_2$, $Ni(NO_3)_2 \cdot 6\ H_2O$ and $BiCl_3$ metal salts. In addition, 1.5 mL of 1 M HCl were added to the Pd and Ni salt solutions for a better solubility. $PdCl_2$ is insoluble in water and forms a square-planar, water soluble complex in the presence of HCl (equation 8) [33]. The solution process of $PdCl_2$ is further accelerated by sonication (Bandelin Sonorex, Typ RK 31H) until complete dissolution.

$$PdCl_2 + 2HCl \rightarrow H_2[PdCl_4] \quad (8)$$

A few drops of concentrated (37 wt.%) HCl were added to the $BiCl_3$ precursor solution instead of 1 M HCl to dissolve the water insoluble bismuth oxychloride (BiOCl) [13].

Afterwards, the metal salt precursor solutions were added to the dispersion of Vulcan XC72R under constant sonication and nitrogen atmosphere in the ice bath. The pH of the mixture is adjusted to 10 by adding 1 M NaOH. The reduction process is carried out by adding $NaBH_4$ (~5 eq., in 6 mL ultrapure water and 0.6 mL of 1 M NaOH) dropwise to the dispersion.

The reaction mixture was stirred at 60 °C for 4 h, whereas nitrogen atmosphere was removed after 1 h. Finally, the catalyst dispersion was cooled to room temperature overnight. The precipitate was filtered instead of centrifuged and was extensively washed several times with ultrapure water. The resulting product was dried at 40 °C overnight and crushed with a mortar to gain a fine, black catalyst powder.

Electrochemical Characterization. The synthesized PdNiBi/C and commercial Pd/C catalysts were ex situ characterized in half-cell experiments. The measurements are performed using a thin film rotating disk electrode (RDE) from PINE Research Instrumentation (AFE5T0GC) in a standard three electrode setup. The RDE, covered with the catalyst, was used as the working electrode, the counter electrode was a platinized titanium rod (Bank Elektronik – Intelligent controls GmbH) and a reversible hydrogen electrode (RHE; Hydroflex®, gaskatel) was utilized as reference electrode. A Reference 600TM Potentiostat/Galvanostat/ZRA and software from GAMRY Instruments was used for data analysis.

The working electrode was prepared by applying the catalyst on a glassy carbon (GC) rotating disk electrode (Ø = 5 mm; 0.196 cm^2) via a suspension. The catalyst powder was mixed with 2-propanol/ultrapure water (7:3) and a Nafion ionomer solution (binder) and was sonicated for 20 minutes to form a homogenous suspension. The GC-RDE was cleaned and polished with an Al_2O_3 powder and rinsed with ultrapure water before each measurement. Two times 5 µL of the suspension are pipetted on the GC-RDE to obtain a Pd-loading of 56 µg cm^{-2}. The electrode was rotated at 700 rpm for 1 h to form a dry, thin and uniform catalyst film.

For the determination of the EASA and the EOR activity (including byproduct tolerance), cyclic voltammetry and EOR measurements were recorded in nitrogen purged potassium hydroxide solution (1 M) and in a mixture of potassium hydroxide and ethanol solution (1 M KOH and 1 M EtOH) at 30 °C with a scan rate of 10 mV s^{-1}. Chronoamperometry (CA) was performed at 0.83 V at 30 °C for 3600 s to examine the stability of the catalysts. Three independent measurements with three cycles for CV and one sweep for CA of each catalyst were recorded and the last cycle with the best performance was used for comparison. The mean value and standard deviation was calculated from all cycles.
The charge of the integrated reduction peak of PdO to Pd (Q_{Pd}; located at 0.65 V - 0.9 V in Figure 4a) was used for the determination of the EASA according to equation 9.

$$EASA = (Q_{Pd}/Q^*_{Pd}) \cdot (1/c_L) \cdot (1/A_{GC}) \quad (9)$$

For the calculations, the assumed value of the reduction charge of PdO to Pd (Q^*_{Pd} = 405 µC cm^{-2}) [13, 34], the catalyst loading of Pd (c_L) and the surface area of the electrode (A_{GC}) are considered.

Results

The EOR performance of the Pd-based nanocatalysts was determined via electrochemical characterization (CV and CA). The results, presented in Figure 3-6, are discussed in this section and summarized in Table 1. In Figure 3, the CV of the PdNiBi/C catalyst recorded in de-aerated 1 M KOH at 30°C in a potential range of 0.05 V – 1.5 V vs. RHE is shown. The characteristic reduction peak V at a potential of 0.5 V – 0.8 V is linked to the reduction of Pd to PdO. Peak III and IV are attributed to the oxidation of $Ni(OH)_2$ to NiOOH and to the reduction of NiOOH to $Ni(OH)_2$ [35]. The oxidation peak II at approx. 0.9 V indicates the formation of Bi_2O_3 from Bi [25]. The associated reduction peak cannot be noticed due to the fact that it is overlapped by the large reduction peak of Pd to PdO. In the lower potential region (peak I), hydrogen ad/absorption is detected [13, 23, 36].

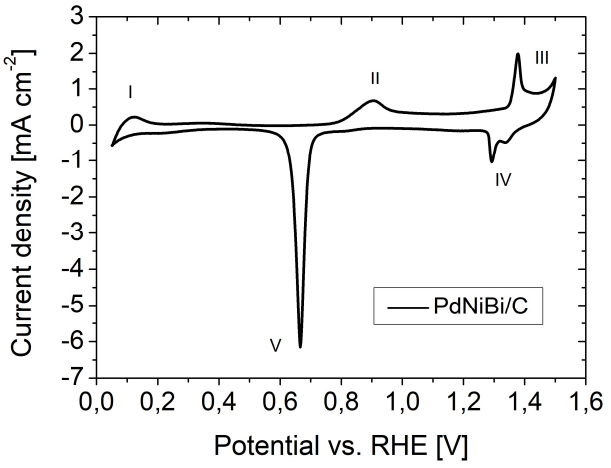

Figure 3: CVs of carbon supported Pd-based nanocatalysts in de-aerated 1.0 M KOH solution at 30 °C with a scan rate of 10 mV s^{-1} from 0.05 V to 1.5 V vs RHE.

Table 1: Electrochemical characterization results of the Pd-based nanocatalysts.

Catalyst	EASA[a] ($cm^2\ mg^{-1}$)	E_{onset}[b] (V)	i_f[c] (mA cm^{-2})	i_b[c] (mA cm^{-2})	i_f/i_b[d]	Q_f/Q_b[e]	i_{rc}[f] (%)
Pd/C	411 ± 21.0	0.255 ± 0.001	126 ± 6.36	150 ± 6.69	0.84 ± 0.07	2.01 ± 0.12	14.5 ± 1.72
PdNiBi/C	636 ± 72.8	0.193 ± 0.008	138 ± 7.23	111 ± 18.3	1.27 ± 0.19	3.29 ± 0.61	27.0 ± 9.84

[a]electrochemical active surface area; [b]E_{onset}, onset potential of the ethanol oxidation; [c]i_f and i_b, peak current density of forward and backward scan; [d]i_f/i_b, byproduct tolerance using peak current density of forward and backward scan; [e]Q_f/Q_b, byproduct tolerance using the charge of the integrated peak current density area of forward and backward scan; [f]i_{rc}, remaining current density after CA at 0.83 V for 3600 s.

The CVs as well as the resulting EASAs of the ternary PdNiBi/C and commercial Pd/C catalyst recorded in de-aerated 1 M KOH at 30°C in a potential range of 0.05 V – 1.2 V vs. RHE are shown in Figure 4. It can be noticed, that the characteristic peak in the negative scan for the reduction of Pd to PdO is much more distinct for the ternary PdNiBi//C catalyst. Therefore, the investigations show a higher EASA of the ternary PdNiBi/C catalyst (636 $cm^2\ mg^{-1}$) compared to the commercial Pd/C catalyst (411 $cm^2\ mg^{-1}$). Furthermore, the presence of Bi reduces the hydrogen ad/absorption on the Pd-based catalyst. This phenomenon can be explained by the strong interaction of Bi with Pd on the catalyst surface [37].

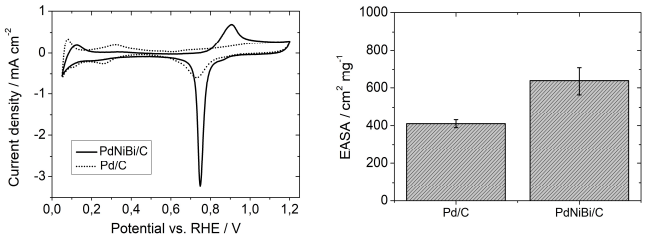

Figure 4: CVs of carbon supported Pd-based nanocatalysts in de-aerated 1.0 M KOH solution at 30 °C with a scan rate of 10 mV s-1 from 0.05 V to 1.2 V (left) and the resulting EASAs (right).

The performance of the Pd-based nanocatalysts for the alkaline EOR is evaluated by cyclic voltammetry in the presence of ethanol. The CVs and the resulting byproduct tolerances toward ethanol reaction intermediates are shown in Figure 5. The onset potential, that is determined at 0.1 mA cm^{-2} and the maximum current density of the forward scan indicate the activity of the catalysts for the alkaline EOR. The ternary PdNiBi/C catalyst shows a lower onset potential (0.193 V) and a higher maximum current density for the forward scan (138 mA cm^{-2}) compared to the commercial Pd/C catalyst (0.255 V, 126 mA cm^{-2}). Furthermore, the maximum current density for the backward scan of the ternary PdNiBi/C (111 mA cm^{-2}) is lower in comparison with the commercial Pd/C catalyst (150 mA cm^{-2}). This indicates a better byproduct tolerance toward ethanol reaction intermediates of the ternary catalyst synthesized by the modified instant method. The calculated byproduct tolerance according to the maximum current densities results in 1.27 for the ternary PdNiBi/C catalyst and in 0.84 for the commercial Pd/C catalyst. The byproduct tolerance determined using the charge of the integrated peak current density area of forward and backward scan leads to the same trend (PdNiBi/C: 3.29, Pd/C: 2.01).

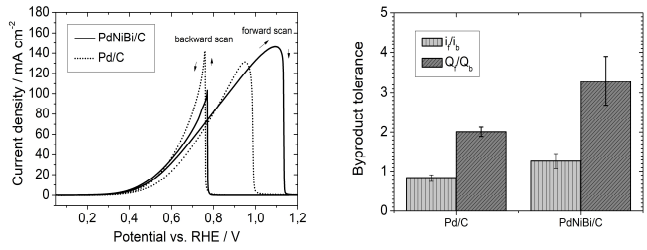

Figure 5: CVs of carbon supported Pd-based nanocatalysts in a mixture of 1.0 M KOH and 1 M EtOH at 30 °C with a scan rate of 10 mV s^{-1} from 0.05 V to 1.2 V (left) and the resulting byproduct tolerances toward ethanol reaction intermediates (right).

The results of the CA measurements and the resulting remaining current densities, to determine the stability of the Pd-based nanocatalysts are shown in Figure 6. The remaining current density of the PdNiBi/C catalyst is 13 % higher compared to the commercial Pd/C catalyst. Moreover, the CA curve of the ternary catalyst indicates a steeper decrease at the beginning of the measurement and afterwards it is more or less stable, whereas the current density of commercial catalyst constantly decreases.

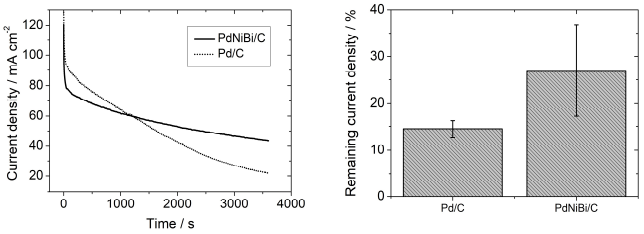

Figure 6: CA measurements for stability determination of the Pd-based nanocatalysts in a mixture of 1.0 M KOH and 1 M EtOH at 30°C at an applied potential of 0.83 V for 3600 s (left) and the resulting remaining current densities (right).

Conclusion

In this work, a ternary PdNiBi/C catalyst was synthesized via the modified instant method. A different purification method (filtering instead of centrifugation) was applied to investigate the influence on the performance for the alkaline EOR. With the CV measurements in a potential range of 0.05 V – 1.5 V, all characteristic reduction and oxidation peaks for Pd, Ni, and Bi as well as for the hydrogen ad/absorption were observed. The results of the electrochemical characterization were compared with a commercial Pd/C catalyst. It was found out that the synthesized PdNiBi/C (636 $cm^2\ mg^{-1}$) catalyst presents a higher EASA than the commercial one (411 $cm^2\ mg^{-1}$) and that the presence of Bi reduces the hydrogen ad/absorption on the Pd-based catalyst. Furthermore, the onset potential of the ternary catalyst (0.193 V, 138 mA cm^{-2}) is lower and the maximum current density of the forward scan is higher compared to the commercial catalyst (0.255 V, 126 mA cm^{-2}). A better byproduct tolerance toward ethanol reaction intermediates of the PdNiBi/C catalyst was examined. The stability tests result in a steeper current density decrease of the commercial catalyst compared to the ternary catalyst and the remaining current density is 13 % lower.

Acknowledgement

Financial support (Project Number: I 3871 International projects) by the Austrian Science Fund (FWF) is gratefully acknowledged.

References

[1] L. Zhang et al., “One-step synthesis of palladium-gold-silver ternary nanoparticles supported on reduced graphene oxide for the electrooxidation of methanol and ethanol,” Electrochim. Acta, vol. 172, pp. 42–51, 2015. https://doi.org/10.1016/j.electacta.2014.11.152

[2] E. Antolini, “Catalysts for direct ethanol fuel cells,” J. Power Sources, vol. 170, no. 1, pp. 1–12, 2007. https://doi.org/10.1016/j.jpowsour.2007.04.009

[3] S. P. S. Badwal, S. Giddey, A. Kulkarni, J. Goel, and S. Basu, “Direct ethanol fuel cells for transport and stationary applications - A comprehensive review,” Appl. Energy, vol. 145, pp. 80–103, 2015. https://doi.org/10.1016/j.apenergy.2015.02.002

[4] L. An, T. S. Zhao, and Y. S. Li, “Carbon-neutral sustainable energy technology: Direct ethanol fuel cells,” Renew. Sustain. Energy Rev., vol. 50, pp. 1462–1468, 2015. https://doi.org/10.1016/j.rser.2015.05.074

[5] J. L. Tan et al., “Preparation and characterization of

palladium-nickel on graphene oxide support as anode catalyst for alkaline direct ethanol fuel cell," Appl. Catal. A Gen., vol. 531, pp. 29–35, 2017. https://doi.org/10.1016/j.apcata.2016.11.034

[6] F. Fathirad, A. Mostafavi, and D. Afzali, "Bimetallic Pd–Mo nanoalloys supported on Vulcan XC-72R carbon as anode catalysts for direct alcohol fuel cell," Int. J. Hydrogen Energy, vol. 42, no. 5, pp. 3215–3221, 2017. https://doi.org/10.1016/j.ijhydene.2016.09.138

[7] M. Z. F. Kamarudin, S. K. Kamarudin, M. S. Masdar, and W. R. W. Daud, "Review: Direct ethanol fuel cells," Int. J. Hydrogen Energy, vol. 38, no. 22, pp. 9438–9453, 2013. https://doi.org/10.1016/j.ijhydene.2012.07.059

[8] K. Kakaei and M. Dorraji, "One-pot synthesis of Palladium Silver nanoparticles decorated reduced graphene oxide and their application for ethanol oxidation in alkaline media," Electrochim. Acta, vol. 143, pp. 207–215, 2014. https://doi.org/10.1016/j.electacta.2014.07.134

[9] R. M. Modibedi, T. Masombuka, and M. K. Mathe, "Carbon supported Pd-Sn and Pd-Ru-Sn nanocatalysts for ethanol electro-oxidation in alkaline medium," Int. J. Hydrogen Energy, vol. 36, no. 8, pp. 4664–4672, 2011. https://doi.org/10.1016/j.ijhydene.2011.01.028

[10] M. A. F. Akhairi and S. K. Kamarudin, "Catalysts in direct ethanol fuel cell (DEFC): An overview," Int. J. Hydrogen Energy, vol. 41, no. 7, pp. 4214–4228, 2016. https://doi.org/10.1016/j.ijhydene.2015.12.145

[11] L. Ma, D. Chu, and R. Chen, "Comparison of ethanol electro-oxidation on Pt/C and Pd/C catalysts in alkaline media," Int. J. Hydrogen Energy, vol. 37, no. 15, pp. 11185–11194, 2012. https://doi.org/10.1016/j.ijhydene.2012.04.132

[12] L. Wang et al., "Energy Efficiency of Alkaline Direct Ethanol Fuel Cells Employing Nanostructured Palladium Electrocatalysts," ChemCatChem, vol. 7, no. 14, pp. 2214–2221, 2015. DOI: 10.1002/cctc.201500189

[13] B. Cermenek et al., "Novel highly active carbon supported ternary PdNiBi nanoparticles as anode catalyst for the alkaline direct ethanol fuel cell," Nano Res., vol. 12, no. 3, pp. 683–693, 2019. https://doi.org/10.1007/s12274-019-2277-z

[14] B. Cermenek, J. Ranninger, V. Hacker; Chapter 15 - Alkaline Direct Ethanol Fuel Cell. In Ethanol: Science and Engineering, A. Basile, A. Iulianelli, F. Dalena, N.T. Veziroglu, Eds.; Amsterdam: Elsevier Inc., pp. 383-405, 2019. https://doi.org/10.1016/B978-0-12-811458-2.00015-8

[15] R. C. Cerritos, M. Guerra-Balcázar, R. F. Ramírez, J. Ledesma-García, and L. G. Arriaga, "Morphological effect of Pd catalyst on ethanol electro-oxidation reaction," Materials (Basel)., vol. 5, no. 9, pp. 1686–1697, 2012. https://doi.org/10.3390/ma5091686

[16] Z. X. Liang, T. S. Zhao, J. B. Xu, and L. D. Zhu, "Mechanism study of the ethanol oxidation reaction on palladium in alkaline media," Electrochim. Acta, vol. 54, no. 8, pp. 2203–2208, 2009. https://doi.org/10.1016/j.electacta.2008.10.034

[17] X. Fang, L. Wang, P. K. Shen, G. Cui, and C. Bianchini, "An in situ Fourier transform infrared spectroelectrochemical study on ethanol electrooxidation on Pd in alkaline solution," J. Power Sources, vol. 195, no. 5, pp. 1375–1378, 2010. https://doi.org/10.1016/j.jpowsour.2009.09.025

[18] C. Bianchini and P. K. Shen, "Palladium-based electrocatalysts for alcohol oxidation in half cells and in direct alcohol fuel cells," Chem. Rev., vol. 109, pp. 4183–4206, 2009. https://doi.org/10.1021/cr9000995

[19] Y. Wang, S. Zou, and W.-B. Cai, "Recent Advances on Electro-Oxidation of Ethanol on Pt- and Pd-Based Catalysts: From Reaction Mechanisms to Catalytic Materials," Catalysts, vol. 5, no. 3, pp. 1507–1534, 2015. https://doi.org/10.3390/catal5031507

[20] L. Bidwell and R. Speiser, "Unit-cell dimensions of Ni-Pd alloys at 25 and 900°C," Acta Crystallogr., vol. 17, no. 11, pp. 1473–1474, 1964. https://doi.org/10.1107/SO365110X64003632

[21] L. Vegard, "Die Konstitution der Mischkristalle und die Raumfüllung der Atome," J. Mater. Sci., vol. 1, no. 1, pp. 79–90, 1921. https://doi.org/10.1007/BF01349680

[22] B. Hammer and J. K. Nørskov, "Theoretical surface science and catalysis - calculations and concepts," Adv. Catal., vol. 45, pp. 71–129, 2000. https://doi.org/10.1016/S0360-0564(02)45013-4

[23] A. O. Neto, M. M. Tusi, N. S. De Oliveira Polanco, S. G. Da Silva, M. Coelho Dos Santos, and E. V. Spinacé, "PdBi/C electrocatalysts for ethanol electro-oxidation in alkaline medium," Int. J. Hydrogen Energy, vol. 36, no. 17, pp. 10522–10526, 2011. https://doi.org/10.1016/j.ijhydene.2011.05.154

[24] J. Cai, Y. Huang, and Y. Guo, "Bi-modified Pd/C catalyst via irreversible adsorption and its catalytic activity for ethanol oxidation in alkaline medium," Electrochim. Acta, vol. 99, pp. 22–29, 2013. https://doi.org/10.1016/j.electacta.2013.03.059

[25] I. G. Casella and M. Contursi, "Characterization of bismuth adatom-modified palladium electrodes. The electrocatalytic oxidation of aliphatic aldehydes in alkaline solutions," Electrochim. Acta, vol. 52, no. 2, pp. 649–657, 2006. https://doi.org/10.1016/j.electacta.2006.05.048

[26] G. J. K. Acres et al., "Electrocatalysts for fuel cells," Catal. Today, vol. 38, pp. 393–400, 1997. https://doi.org/10.1016/S0920-5861(97)00050-3

[27] M. Kim, J. N. Park, H. Kim, S. Song, and W. H. Lee, "The preparation of Pt/C catalysts using various carbon materials for the cathode of PEMFC," J. Power Sources, vol. 163, no. 1 SPEC. ISS., pp. 93–97, 2006. https://doi.org/10.1016/j.jpowsour.2006.05.057

[28] X. Yu and S. Ye, "Recent advances in activity and durability enhancement of Pt/C catalytic cathode in PEMFC. Part I. Physico-chemical and electronic interaction between Pt and carbon support, and activity enhancement of Pt/C catalyst," J. Power Sources, vol. 172, no. 1, pp. 133–144, 2007. https://doi.org/10.1016/j.jpowsour.2007.07.049

[29] E. D. Wang, J. B. Xu, and T. S. Zhao, "Density functional theory studies of the structure sensitivity of ethanol oxidation on palladium surfaces," J. Phys. Chem. C, vol. 114, no. 23, pp. 10489–10497, 2010. https://doi.org/10.1021/jp101244t

[30] D. Hao et al., "Synthesis of monodisperse palladium nanocubes and their catalytic activity for methanol electrooxidation," Chinese Phys. B, vol. 19, no. 10, p. 106104, 2010. http://www.iop.org/journals/cpb

[31] K. I. Ozoemena, "Nanostructured platinum-free electrocatalysts in alkaline direct alcohol fuel cells: Catalyst design, principles and applications," RSC Adv., vol. 6, no. 92, pp. 89523–89550, 2016. DOI: 10.1039/c6ra15057h

[32] Q. Shen et al., "Morphology-Controlled Synthesis of Palladium Nanostructures by Sonoelectrochemical Method and Their Application in Direct Alcohol Oxidation," J. Phys. Chem. C, vol. 113, no. 4, pp. 1267–1273, 2009. https://doi.org/10.1021/jp807881s

[33] B. Cermenek et al., "Alkaline Ethanol Oxidation Reaction on Carbon Supported Ternary PdNiBi

Nanocatalyts using Modified Instant Reduction Synthesis Method," Electrocatalysis, vol. 11, pp. 203–214, 2020. https://doi.org/10.1007/s12678-019-00577-8

[34] S. Jongsomjit, P. Prapainainar, K. Sombatmankhong, "Synthesis and characterisation of Pd-Ni-Sn electrocatalyst for use in direct ethanol fuel cells," Solid State Ionics, vol. 288, pp. 147–153, 2016. https://doi.org/10.1016/j.ssi.2015.12.009

[35] Z. Zhang, L. Xin, K. Sun, W. Li, "Pd-Ni electrocatalysts for efficient ethanol oxidation reaction in alkaline electrolyte," Int. J. Hydrogen Energy, vol. 36, pp. 12686–12697, 2011. https://doi.org/10.1016/j.ijhydene.2011.06.141

[36] R.N. Singh, A. Singh, Anindita, "Electrocatalytic activity of binary and ternary composite films of Pd, MWCNT, and Ni for ethanol electro-oxidation in alkaline solutions," Carbon, vol. 47, pp. 271–278, 2009. https://doi.org/10.1016/j.carbon.2008.10.006

[37] M. Simões, S. Baranton, C. Coutanceau, "Influence of bismuth on the structure and activity of Pt and Pd nanocatalysts for the direct electrooxidation of NaBH4," Electrochim. Acta, vol. 56, pp. 580–591, 2010. https://doi.org/10.1016/j.electacta.2010.09.006